RSC Advances

PAPER

View Article Online
View Journal | View Issue



Cite this: *RSC Adv.*, 2016, **6**, 88050

# Iron piano-stool complexes containing NHC ligands outfitted with pendent arms: synthesis, characterization, and screening for catalytic transfer hydrogenation†

Parthapratim Das,[a] Thomas Elder,[b] William W. Brennessel[c] and Stephen C. Chmely*[a]

Received 17th August 2016
Accepted 7th September 2016

DOI: 10.1039/c6ra20764b

www.rsc.org/advances

Two iron piano-stool complexes containing NHC ligands equipped with hydroxyl-containing pendent arms (aliphatic and aromatic) have been prepared *via* deprotonation of the imidazolium salts with a strong base. Access to the anionic ligand is afforded with an additional equivalent of base when the wingtip contains a bulky phenol group. X-ray crystallography and DFT calculations demonstrate an apparent delocalization of the resulting negative charge, which evidently stabilizes the complex. The strongly donating ligands affect the electronic environment at the Fe center to a degree measurable using FTIR spectroscopy. The complexes were screened for catalytic transfer hydrogenation of benzaldehyde, acetophenone and benzophenone using 2-propanol as a solvent and hydrogen donor. The molecular complexes under visible light do not show reactivity towards reduction of carbonyls. Attempts to boost catalyst turnover under *in situ* conditions using UV light resulted in an unwanted photo-induced pinacolization of acetophenone in both cases and decomposition of the aromatic-containing NHC complex to an iron mirror.

## Introduction

Catalysis is a fundamental technology that is widely used in the food, petrochemical, pharmaceutical, and agricultural sectors to produce chemical products on an industrial scale. Well-defined molecular organometallic species are a cornerstone of catalytic methodology, and the activity and selectivity of these complexes can be modulated by judicious choice of metal and surrounding ligands. Catalysts containing precious metals such as Pd, Rh, Ir, and Ru are typically very efficient, as related reactions require extremely low catalyst loadings. However, precious metals have very limited availability and are subsequently rather expensive. In addition, complexes of these metals can be toxic. Accordingly, a vast body of recent research has focused on the use of "cheap metals for noble tasks".[1] One particularly attractive target is iron,[2] since it is the second-most abundant metal (after aluminum) in the Earth's crust.[3] Moreover, iron is present in a number of metalloproteins and complexes of iron are relatively nontoxic. The availability of multiple oxidation states makes iron even more lucrative for redox transformations.

N-heterocyclic carbenes (NHCs) are isolable nitrogen-containing heterocycles that contain a neutral carbon atom bearing six valence electrons. These species are attractive as ligands for transition metal catalysis for a number of reasons. First, they are electron rich, neutral σ-donor ligands. In fact, NHCs tend to be more basic than even the most electron-donating phosphine ligands.[4] In addition, transition metal NHC complexes are generally very robust, and they resist decomposition due to heat, air, and moisture.[5] Finally, NHCs are sterically demanding ligands that can encapsulate a metal center and impart unique reactivity to catalysts.

The first NHC complexes of iron were synthesized in the 1970s,[6–9] and investigations into the use of Fe–NHC complexes as catalysts have rapidly increased in the past decade.[10–12] Fe–NHC complexes have shown to be involved in hydroboration of alkenes,[13] hydroxylation of benzene and toluene,[14] C–C cross coupling[15] and more recently in double carbometallation reactions.[16] Moreover, they have been reported extensively for catalytic hydrosilylation of C = X (X = heteroatom) bonds. In fact, there are a variety of NHC complexes of Fe that have been shown to catalyze hydrosilylation, including complexes containing NHC-tethered Cp ligands,[17–19] a square-planar bis-NHC complex,[20] an NHC–Fe(0) complex,[21,22] Fe complexes of NHCs bearing a malonate or an imidate backbone,[23] various iron

[a]*Center for Renewable Carbon, University of Tennessee, Knoxville, Tennessee 37996, USA. E-mail: schmely@utk.edu*

[b]*USDA-Forest Service, Southern Research Station, Auburn, Alabama 36849, USA*

[c]*X-ray Crystallographic Facility, Department of Chemistry, University of Rochester, Rochester, New York 14627, USA*

† Electronic supplementary information (ESI) available: NMR spectra of compounds, reaction yields and optimized Cartesian coordinates for all computed structures. CCDC 1441263 and 1441264. For ESI and crystallographic data in CIF or other electronic format see DOI: 10.1039/c6ra20764b

piano-stool NHC complexes.[24–30] and complexes formed *in situ*.[31,32] There are also few reports on iron NHC-catalyzed transfer hydrogenations of ketones have been published recently.[17,20,33]

The steric nature of NHC ligands can be easily tuned by alteration of the wingtip substituents and subsequently the electronic nature of the metal center in organometallic complexes containing these ligands is modulated. In this work, we report on a pair of NHC-containing piano-stool complexes of iron. The NHC ligands are outfitted with pendent arms containing hydroxyl or phenol groups, which we demonstrate have a measureable effect on the electronic environment at the metal center using IR spectroscopy and DFT calculations. The solid-state behavior of these complexes was also investigated using single-crystal X-ray diffractometry. Finally, as part of these investigations, we have screened these species as catalysts for the transfer hydrogenation of benzaldehyde, acetophenone, and benzophenone. The results reported here suggest that the compounds are not active for transfer hydrogenation of carbonyls, although we are able to speculate on this lack of reactivity.

## Results and discussion

Compound **1** was prepared following a procedure as described previously (Scheme 1).[34] Reaction of 1-methylimidazole and 2-bromoethanol affords the target imidazolium bromide in near quantitative yield. The white powder matches previously reported spectroscopic data, and the elemental analysis is in agreement with the target compound.

Compound **2** was also prepared following a published literature procedure (Scheme 2).[35] Curiously, formation of **2** only occurs in the presence of ethylene glycol, whereas substitution at the 4 position in the dienone occurs in its absence. NMR spectra and elemental analysis confirm the presence of **2**, although the yield of the compound is rather low (25%).

Treatment of **1** with one equivalent of KOtBu followed by treatment with cyclopentadienyliron dicarbonyl iodide (FpI) afforded the piano-stool complex **3** in moderate yield (Scheme 3). The complex was isolated as a crystalline yellow solid, and its identity was established by analytical and spectroscopic methods. The $^1$H NMR spectrum displays the expected pattern for complex **3**. There are two peaks associated with the cyclopentadienyl protons (4 : 1 ratio), which could indicate a slight barrier to free rotation of the Cp ring at ambient temperature. We were unable to detect the hydroxyl proton in the $^1$H NMR spectrum.

X-ray-quality crystals of **3** were obtained by solvent layering and were characterized by single-crystal X-ray diffractometry (Fig. 1). Complex **3** adopts a piano-stool arrangement that is characteristic of half-sandwich iron complexes. The iodide has been displaced from the inner to the outer coordination sphere of the complex by the carbene ligand. There is one co-crystallized molecule of dichloromethane per cation–anion pair in the unit cell. The Fe–carbene distance of 1.969(3) Å is within the expected range for complexes of this type.[36] The CO–Fe–CO bond angle of 90.8(1)° is smaller than the two CO–Fe–carbene bond angles (95.8(1)° and 93.7(1)°), which is indicative of the steric congestion imparted by the bulky NHC ligand. The Fe–O3 distance of 4.234(3) Å indicates that the oxygen is outside the coordination sphere of iron.

We attempted to isolate the compound analogous to **3** using imidazolium salt **2** and one equivalent KOtBu as is outlined in Scheme 3. However, these attempts afforded a complex mixture of compounds. We were able to detect cyclopentadienyliron

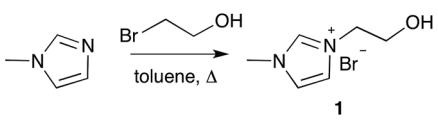


Scheme 1 Synthesis of compound **1**.

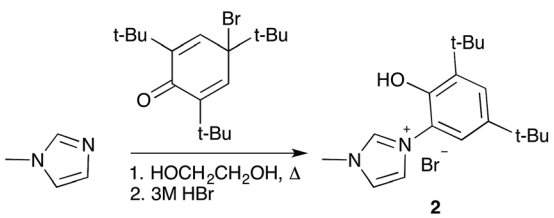


Scheme 2 Synthesis of compound **2**.

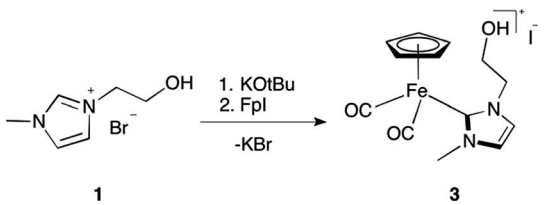


Scheme 3 Synthesis of compound **3**.

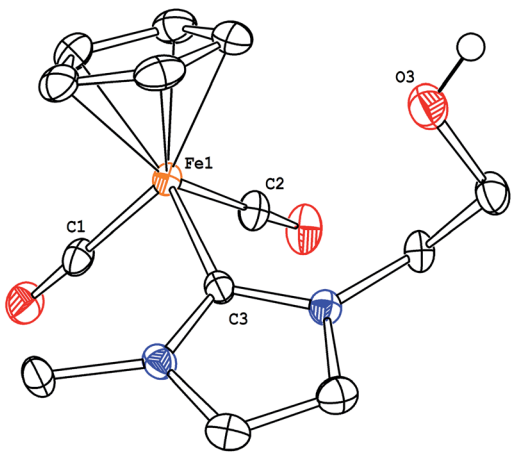


Fig. 1 ORTEP drawing of the organometallic cation fragment in **3**. Displacement ellipsoids are at the 50% probability level. H-atoms (except for the hydroxyl-H), I-atom, and co-crystallized dichloromethane have been omitted for clarity. Selected interatomic distances (Å): Fe1–C1 = 1.776(3), Fe1–C2 = 1.774(3), Fe1–C3 = 1.969(3).

dicarbonyl dimer ($Fp_2$) using $^1H$ NMR spectroscopy, but were unable to otherwise characterize this mixture. However, treatment of **2** with two equivalents of KOtBu followed by treatment with FpI affords zwitterion **4** in moderate yield (Scheme 4). The complex was isolated as a red-orange crystalline solid, and its identity was established by analytical and spectroscopic methods. Elemental analysis confirms the absence of any halogens, and **4** is readily studied using NMR spectroscopy. Given that use of an additional equivalent of KOtBu promotes the formation of the zwitterion, we hypothesize that the sub-stoichiometric reaction (1 equivalent KOtBu) affords 0.5 equivalents of **4** and 0.5 equivalents of starting materials.

X-ray quality crystals of **4** were obtained by solvent layering and were characterized by single-crystal X-ray diffractometry (Fig. 2). In a manner similar to **3**, complex **4** adopts the expected piano-stool arrangement. Complex **4** does not contain a non-coordinating anion. The Fe–carbene distance of 1.973(1) Å is slightly longer than that of **3**, indicating the increased steric congestion at iron. As in the case of **3**, the Fe–O3 distance of 4.1291(9) Å reveals that the O-atom lies outside the coordination sphere of the Fe-atom.

The O3–C12 distance of 1.289(1) Å is shorter than expected for a C–O(H) bond (1.43 Å) but longer than a C=O bond (1.23 Å). Moreover, C7–C12 and C11–C12 (1.429(2) Å and 1.447(2) Å, respectively) are slightly longer than expected for a C–C bond in an aromatic ring (1.40 Å) but shorter than a C–C single bond (1.47 Å). These data suggest that the negative charge at O3 has been delocalized into the π-orbitals of the aromatic ring.

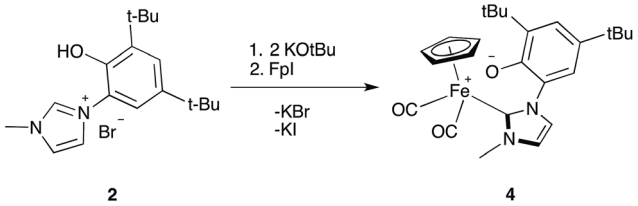


2 4

Scheme 4 Synthesis of compound **4**.

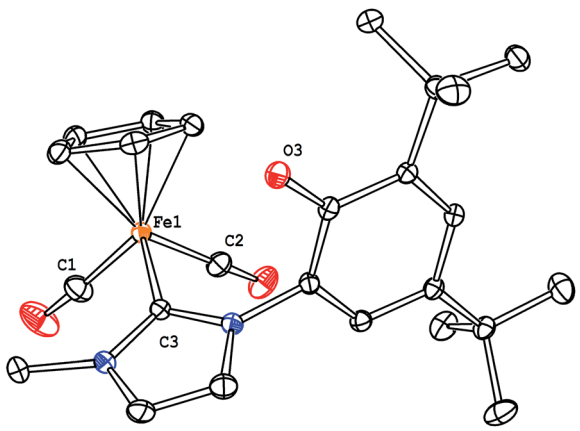


Fig. 2 ORTEP drawing of the organometallic zwitterion **4**. Displacement ellipsoids are at the 50% probability level. H-atoms have been omitted for clarity. Selected interatomic distances (Å): Fe1–C1 = 1.767(1), Fe1–C2 = 1.776(1), Fe1–C3 = 1.973(1).

FTIR spectroscopy was used to probe the electronic nature of the complexes by monitoring the CO stretching frequencies of **3** and **4** in solution. These values can be compared to those of known piano-stool Fe–NHC complexes,[33] and the results are displayed in Table 1. Whereas the identity of the R-groups when R is an alkane has no demonstrable effect on the donor properties of the NHC ligand,[26] the CO stretching frequencies in **3** are 14–16 $cm^{-1}$ lower than those in the two structurally related compounds, which indicates that the O-containing pendent arm imparts enhanced basicity to the NHC ligand. Moreover, the CO stretching frequencies in **4** are lower still, indicating the greatly enhanced basicity of the deprotonated aromatic pendent sidearm.

We performed DFT calculations (see Computational details) to determine the effects the ligands have on the electronic environment of the metal complexes. Specifically, we were interested in elucidating the reasons for our ability to isolate complex **4** but not the related zwitterion of **3**. The calculated structures for **3** and **4** were in good agreement with the crystal structure data at the level of theory used. Deprotonation of **3** *in silico* affords the related zwitterion **3z**, and a graphical comparison of its highest occupied molecular orbital (HOMO) to the HOMO of **4** is depicted in Fig. 3. Whereas the negative charge in **3z** is confined almost entirely to an orbital that is antibonding with respect to the C–O bond in the pendent arm, the negative charge in **4** has been delocalized onto the phenyl ring. The associated changes in bond lengths are evident in the crystal structure of **4** as well. The significant delocalization of the negative charge in **4** can be used to explain its relative thermodynamic stability, which contributes to its isolability.

We were interested in probing the reactivity of the complexes **3** and **4** towards catalytic transfer hydrogenation (CTH) of

Table 1 Comparison of CO stretching frequencies

| Complex | $\nu$(CO)/$cm^{-1}$ |
|---|---|
| $R_1 = R_2 = Me$ | 2048, 2000 |
| $R_1 = Me$, $R_2 = Et$ | 2047, 2000 |
| **3** | 2033, 1984 |
| **4** | 1993, 1930 |

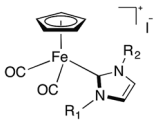


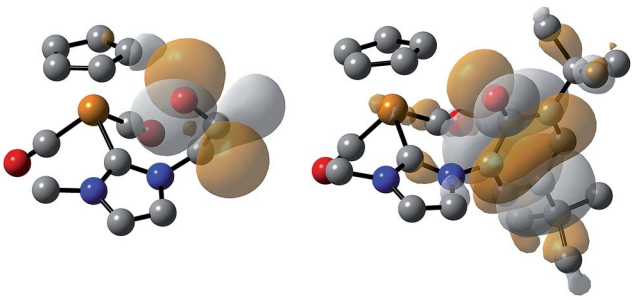

Fig. 3 Boundary surfaces of the calculated highest occupied molecular orbitals of the putative zwitterion **3z** (left) and the isolated complex **4** (right). H-atoms have been omitted for clarity.

carbonyls using 2-propanol as a solvent and hydrogen donor. We were intrigued by the possibility that the presence of a hydroxylated pendant arm might assist in proton transfer from 2-propanol *via* an outer sphere mechanism.[37] Accordingly, we have tested the ability of **3** and **4** to mediate the transfer hydrogenation of benzaldehyde, acetophenone, and benzophenone under visible light irradiation. Reaction progress was monitored using GC/MS, and product quantifications were made by constructing appropriate response factor curves.

Unfortunately, no reduction products were observed when complexes **3** and **4** (10 mol%) were allowed to react with acetophenone and benzophenone at 75 °C for 15 hours under visible light in the presence of KOH. Not surprisingly, a reaction between complex **4** and acetophenone under base-free conditions also did not yield 1-phenylethanol. In the case of benzaldehyde, negligible amounts of benzyl alcohol were observed with either of the complexes and KOH. A control reaction (in the absence of iron) under identical condition involving KOH and benzaldehyde also yielded benzyl alcohol, which could be obtained either *via* reduction or *via* the disproportionation (Cannizzaro) reaction, which produces 0.5 eq. each of the related alcohol and acid, the latter being undetectable using the GC column we employed.

Interestingly, reactivity for transfer hydrogenation of a number of polar double bonds has been demonstrated using catalyst species generated *in situ* from FpI, an appropriate imidazolium salt, and KOH.[33] Therefore, we set to test the reactivity of the complexes generated *in situ* from FpI and **1** or **2**. We used a methodology similar to one presented previously by Bala *et al.*[33] In a typical experiment, FpI, imidazolium salt, KOH, and acetophenone were added to freshly distilled 2-propanol such that the resulting solution contained 5 mol% Fe. The reactor was sealed and heated to 80 °C for 16 h. We also conducted a blank test, where products were monitored in the absence of Fe and imidazolium salt, to determine the amount of conversion due to KOH alone.

For the blank reaction, we noted 56% conversion of acetophenone and a 44% yield of 1-phenylethanol (selectivity of 79%, see ESI for further details†). This result is in agreement with previous reports of alkali-metal hydroxides catalysing the transfer hydrogenation of ketones to alcohols using 2-propanol as the reductant.[38,39] We were unable to detect any other products *via* GC/MS. We noted essentially identical reactivity when **1** and FpI were used as pre-catalysts, with 56% conversion of acetophenone and 39% yield of 1-phenylethanol (70% selectivity). However, *in situ* CTH using **2** and FpI affords >99% conversion of acetophenone and quantitative yield of 1-phenylethanol (>99% selectivity).

The obtained results are inconclusive and do not clearly indicate the involvement of iron-mediated CTH. Furthermore, a CTH mechanism involving the thermodynamically stable, 18-electron complexes **3** and **4** is difficult to envision, since those as-isolated complexes do not contain open coordination sites for catalytic activation of 2-propanol or acetophenone. The inactivity of the complexes towards CTH is evidently a result of the coordinative saturation around iron. Furthermore, binding of the strongly σ-donating NHC ligands to the iron atom enhances Fe–C(O) d–π* back-donation. The extent of the back-donation increases with an increase in the basicity of the sidearm, as exemplified by decreasing CO stretching frequencies (Table 1). This results in a marked decrease in lability of CO ligands when compared to iron complexes that contain NHC ligands with identical wingtips.

In spite of previous reports of catalytic hydrosilylation of carbonyls using similar Fe–NHC complexes under visible light from a compact fluorescent lamp,[24,27,40] we did not observe any transfer hydrogenation products using molecular complexes **3** and **4** under visible light. As a result, we investigated the possibility of generating a catalytically active species *in situ* by decarbonylation of the pre-catalyst **3** or **4** using UV light (Scheme 5). We hypothesized that a complex such as **4′** could participate in CTH *via* an outer-sphere mechanism,[37] whereby transfer of proton and hydride occurs with assistance from the phenoxide sidearm and the coordinatively unsaturated Fe, respectively.

For UV-assisted CTH, we used identical reaction conditions and a specially designed quartz micro reactor that is equipped with a handheld low-pressure Hg gaseous discharge lamp that operates at 254 nm. The lamp is inserted into a jacketed quartz dip tube that is then immersed in the reaction mixture to maximize the exposure of the reactants to UV photons. The results of these reactions are summarized in the ESI.†

In the case of UV-assisted CTH with compound **1**, quantitative conversion of acetophenone is observed. However, only 40% yield of 1-phenylethanol is obtained. In addition to 1-phenylethanol, we were able to detect 2,3-diphenylbutane-2,3-diol using GC/MS. The photo-induced pinacolization of acetophenone has been shown to occur in 2-propanol with 80% yield after 6–9 h;[41] evidently this reaction is occurring in competition with CTH to afford 1-phenylethanol. In contrast, conversion of acetophenone in the presence of **2** decreases in the presence of UV light. A 77% conversion of acetophenone was obtained with a concomitant 22% yield of 1-phenylethanol. Again, we were able to detect the pinacol product, suggesting that photo-pinacolization and CTH occur competitively. In addition, we noted a metallic mirror formed on the quartz dip tube after completion of the reaction. This suggests that the catalytic complex formed form FpI and **2** is unstable to UV photons and decomposes to iron metal. This is consistent with previous reports of UV-assisted reactions to afford metallic thin films from the associated metal carbonyls.[42] The lower yield of and selectivity for 1-phenylethanol is apparently attributable to decomposition of the catalyst species. A preliminary attempt to isolate the mono-carbonyl complexes of iron from **4** under UV light led to the formation of an orange solid, not soluble in any organic solvents.

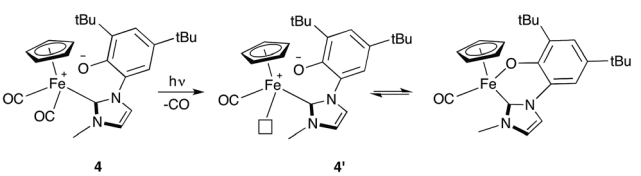


Scheme 5 Putative UV-assisted decarbonylation of **4**.

## Conclusions

In summary, we have described the preparation of a pair of piano-stool Fe complexes outfitted with NHC ligands containing hydroxyl-appended pendent arms. An organometallic zwitterion is accessible by double deprotonation of the NHC ligand with strong base when the wingtip contains an aromatic ring, which serves to delocalize the negative charge and stabilize the resulting complex. FTIR spectroscopy elucidates the enhanced basicity of these ligand systems. The screening of iron complexes did not show any activity towards transfer hydrogenation of benzaldehyde, acetophenone, nor benzopheone using 2-propanol as the solvent and reductant. Attempts to observe catalytic activity under *in situ* reaction conditions by decarbonylation using UV light affords a photo-induced pinacolization of acetophenone as expected, as well as an unexpected decomposition of the catalyst species. Any conversion of carbonyl to alcohol could be explained by Meerwein–Ponndorf–Verley reduction of the substrates in the presence of KOH, and is unlikely due to catalytic mediation of dicarbonyl complexes such as **3** or **4**. Further attempts to isolate and characterize the mono-carbonyl iron species, which could display catalytic reactivity, are ongoing in our laboratory.

## Experimental

### Materials and methods

Unless otherwise stipulated, all manipulations were performed with the rigorous exclusion of air and moisture using Schlenk or glovebox techniques. All solvents were dried and purified using a solvent purification system or using other standard methods before use. Reagents were obtained from Sigma-Aldrich (St. Louis, MO) unless noted otherwise and were used as received. KOH (85% purity) was obtained from Fisher Scientific (Waltham, MA). $^{1}$H (400 MHz) and $^{13}$C{$^{1}$H} (100 MHz) NMR spectra were collected using a Varian Unity 400 MHz NMR spectrometer at ambient temperature. Chemical shifts have been referenced relative to residual solvent peaks. Fourier-transformed IR spectra were collected using a Thermo Scientific Nicolet IR-100 FTIR spectrometer. The products of catalytic screening reactions were identified using an Agilent 7890B GC system (Agilent HP-5ms capillary column) coupled to an Agilent 5977A MSD. Elemental analyses were performed by Atlantic Microlab Inc. (Norcross, GA). The complex 4-bromo-2,4,6-tri-*tert*-butylcylcohexa-2,5-dien-1-one was synthesized according to a published literature procedure.[35]

**Synthesis of 3-(2-hydroxyethyl)-1-methyl-1*H*-imidazol-3-ium bromide (Me–NHC–EtOH, 1).** Compound **1** was prepared with modifications to a published procedure.[20] No attempts were made to exclude air from the reaction. A toluene solution of 1-methylimidazole (2.0 mL, 25 mmol) and 2-bromoethanol (1.9 mL, 25 mmol) was refluxed for 14 hours. After cooling to ambient, the flask was stored at −10 °C for 48 hours to afford a white solid. The solid was filtered, washed with 30 mL hexanes, and dried under vacuum (4.66 g, 90.0%). $^{1}$H NMR (DMSO-$d_6$, 400 MHz): $\delta$ 9.17 (s, ImH, 1H), 7.76 (dd, $J$ = 3.6 Hz, $J$ = 2 Hz, CH═CH, 1H), 7.72 (dd, $J$ = 3.6 Hz, $J$ = 2 Hz, CH═CH, 1H), 5.15 (broad, $CH_2CH_2OH$, 1H), 4.23 (t, $J$ = 5.6 Hz, $CH_2$-$CH_2OH$, 2H), 3.87 (s, $NCH_3$, 3H), 3.71 (t, $J$ = 5.6 Hz, $CH_2CH_2OH$, 2H) ppm. $^{13}$C{$^{1}$H} NMR (DMSO-$d_6$, 100 MHz): $\delta$ 136.7 (im-CH), 123.3 (im-C═C), 122.6 (im-C═C), 59.2 (N–$CH_2CH_2OH$), 51.5 (N–$CH_2CH_2OH$), 35.65 (*N*-methyl). Anal. calcd (found) for **1** $2.5H_2O$ $C_6H_{16}BrN_2O_{3.5}$: C 28.59 (28.21), H 6.40 (6.27) N 11.11 (10.64).

**Synthesis of 3-(3,5-di-*tert*-butyl-2-hydroxyphenyl)-1-methyl-1*H*-imidazol-3-ium bromide (Me–NHC-ArOH, 2).** Compound **2** was prepared according to a published procedure.[21] No attempts were made to exclude air from the reaction. A solution of 1-methylimidazole (1.6 mL, 20 mmol) and 4-bromo-2,4,6-tri-*tert*-butylcyclohexa-2,5-dien-1-one (3.46 g, 10.1 mmol) in ethylene glycol (0.56 mL, 10 mmol) was heated at 135 °C for 8 h. Then, a 3 M solution of HBr was added and the resulting suspension was vigorously stirred and filtered. The obtained crude solid was washed with water (3 × 10 mL) and hexanes (3 × 20 mL) to yield a white solid (0.91 g, 25.0%). $^{1}$H NMR (DMSO-$d_6$, 400 MHz): $\delta$ 9.45 (s, ArO*H*, 1H), 9.14 (s, Im*H*, 1H), 7.91 (m, Ar–*H*, 1H), 7.88 (m, Ar–*H*, 1H), 7.41 (d, $J$ = 4 Hz, im-C*H*, 1H), 7.27 (d, $J$ = 4 Hz, im-C*H*, 1H), 3.93 (s, N$CH_3$, 3H), 1.41 (s, *tert*-butyl, 9H), 1.28 (s, *tert*-butyl, 9H) ppm. $^{13}$C{$^{1}$H} NMR (DMSO-$d_6$, 100 MHz): $\delta$ 147.4 (im-*C*H), 142.3 (Ar–*C*), 139.3 (Ar–*C*), 138.2 (Ar–*C*), 125.2 (Ar–*C*), 124.4 (Ar–*C*), 124.1 (Ar–*C*), 123.5 (im-C═*C*), 121.6 (im-*C*═C), 35.7 (methyl of *tert*-butyl), 35.1 (methyl of *tert*-butyl), 34.1 (methyl of *tert*-butyl), 31.1 (*N*-methyl), 29.5 (tertiary carbon of *tert*-butyl). Anal. calcd (found) for **2** $C_{18}H_{27}BrN_2O$: C 58.86 (58.66), H 7.41 (7.35) N 7.63 (7.52).

**Synthesis of [CpFe(Me–NHC–EtOH)(CO)$_2$]I (3).** KOtBu (0.309 g, 2.76 mmol, 1.1 equiv.) was added to a stirring suspension of **1** (0.519 g, 2.51 mmol, 1.0 equiv.) in THF. The resulting mixture was allowed to stir for 1 h, after which time $CpFe(CO)_2I$ (0.647 g, 2.13 mmol, 0.85 equiv.) in THF was added dropwise. The resulting mixture was allowed to stir overnight. Diethyl ether was added and the resulting mixture was filtered. The filtrate was collected, concentrated to dryness, and re-dissolved in dichloromethane. This solution was subsequently layered with diethyl ether and allowed to stand overnight to afford semi-crystalline solid. Upon recrystallization using the same solvent mixture a crop of light-yellow X-ray-quality crystals of **3** was obtained (0.22 g, 20.0%). NMR spectra have been collected by dissolving the obtained crystals in $CD_3CN$ while the solid was used for elemental analysis. $^{1}$H NMR ($CD_3CN$, 400 MHz): $\delta$ 7.48 (d, $J$ = 2 Hz, C*H*═CH, 1H), 7.35 (d, $J$ = 2 Hz, CH═C*H*, 1H), 5.45 (s, *Cp*, 1H), 5.32 (s, *Cp*, 4H), 4.25 (t, $J$ = 4 Hz, N$CH_2CH_2$, 2H), 3.89 (dd, $J$ = 8, 4 Hz, $NCH_2CH_2$, 1H), 3.78 (s, N$CH_3$, 3H), 3.39 (t, $J$ = 5 Hz, 1H). $^{13}$C{$^{1}$H} NMR ($CD_3CN$, 100 MHz): $\delta$ 211.3 (CO), 126.3 (im), 124.0 (im), 86.8 (Cp), 59.8 ($CH_2CH_2OH$), 52.7 ($CH_2CH_2$-OH), 45.8 ($CH_3$). IR ($CH_2Cl_2$, cm$^{-1}$) 2033 $\nu$(CO), 1984 $\nu$(CO). Anal. calcd (found) for **3** $C_{13}H_{16}FeIN_2O_3\cdot CH_2Cl_2$: C 32.70 (32.60), H 3.33 (3.32) N 6.44 (6.47).

**Synthesis of [CpFe(CO)$_2$]$^+$[Me–NHC-ArO]$^-$ (4).** KOtBu (0.109 g, 0.971 mmol, 2.12 equiv.) was added to a stirring suspension of **2** (0.168 g, 0.457 mmol, 1.0 equiv.) in THF. The resulting mixture was allowed to stir for 1 h at ambient and was subsequently cooled to 0 °C. Then, a pre-cooled (0 °C) THF solution of $CpFe(CO)_2I$ (0.115 g, 0.378 mmol, 0.83 equiv.) was added and

 

the resulting mixture was allowed to warm to ambient and stir for 1 h. The resulting mixture was filtered and the filtrate was collected and concentrated to dryness to afford an orange oil. The oil was dissolved in dichloromethane, layered with diethyl ether, and allowed to stand to afford red-orange solid (used for elemental analysis). X-ray-quality crystals have been obtained during recrystallization using the aforementioned solvent mixture (0.052 g, 30.0%) and used for NMR analysis. $^1$H NMR ($CDCl_3$, 400 MHz): 7.51 (s, im-*H*, 1H), 7.11 (s, im-*H*, 1H), 7.00 (s, Ar–*H*, 1H), 6.94 (s, Ar–*H*, 1H), 5.28 (s, Cp-*H*, 1H), 4.49 (s, Cp-*H*, 4H), 3.69 (s, C*H*$_3$, 3H), 1.29 (s, *t*-butyl, 9H), 1.26 (s, *t*-butyl, 9H). $^{13}$C{$^1$H} NMR ($CDCl_3$, 100 MHz): $\delta$ 223.3 (CO), 123.8 (aryl), 121.3 (im), 120.1 (im), 113.4 (aryl), 81.2 (Cp), 35.7 (methyl), 32.0 (*tert*-butyl), 30.0 (*tert*-butyl). IR ($CH_2Cl_2$, cm$^{-1}$) 1993 $\nu$(CO) 1930 $\nu$(CO). Anal. calcd (found) for **4** $(CH_2Cl_2)_2$ $C_{28}H_{38}Cl_4FeN_2O_3$: C 51.21 (50.91), H 5.57 (5.93) N 4.42 (5.28).

### Structural determination of 3 and 4

All data collection and structure solutions for both molecules were conducted at the X-ray Crystallography Facility at the University of Rochester by Dr William W. Brennessel. Data for compounds **3** and **4** were collected on a Bruker SMART Platform diffractometer equipped with an APEX II CCD area detector with use of monochromated MoK$\alpha$ radiation (graphite monochromator) with a frame time of 25 s (**3**) or 45 s (**4**) and a detector distance of 4.00 cm (**3**) or 4.04 cm (**4**). The structures were solved using SIR2011 and refined using SHELXL-2014 for full-matrix, least-squares refinement against $F^2$. All H atoms were placed in ideal positions and refined as riding atoms with relative isotropic displacement parameters. Data collection parameters and crystallographic information are given in Table 2.

### Computational methodology

All calculations were performed using the GAUSSIAN 09 software package[43] at the M06-2X[44] level of theory using the fine integration grid, consisting of 75 radial shells and 302 angular points per shell. A mixed basis set using 6-311++G(d, p) for C, H, N, and O and the LANL2DZ basis set for Fe was employed. The single-crystal X-ray structures described in this work were used to build the models for geometry optimizations. No symmetry constraints were applied, and no imaginary frequencies were found, indicating the optimized structures are true stationary minima.

Table 2 Crystallographic data for complexes **3** and **4**

| | **3** | **4** |
|---|---|---|
| Formula | $C_{14}H_{17}Cl_2FeIN_2O_3$ | $C_{25}H_{30}FeN_2O_3$ |
| $F_w$ | 514.95 | 462.36 |
| $T$ (K) | 100.0(5) | 100.0(5) |
| Space group | *Fdd*2 | $P2_1/n$ |
| $a$ (Å) | 29.269(4) | 10.8596(11) |
| $b$ (Å) | 38.689(5) | 8.8254(9) |
| $c$ (Å) | 6.4704(9) | 23.959(3) |
| $\alpha$ (°) | 90 | 90 |
| $\beta$ (°) | 90 | 101.211(2) |
| $\gamma$ (°) | 90 | 90 |
| $V$ (Å$^3$) | 7327.01(17) | 2252.4 |
| $Z$ | 16 | 4 |
| $\rho$ (mg m$^3$) | 1.867 | 1.363 |
| Refl collected | 68 174 | 54 838 |
| Unique refl | 9897 | 12 380 |
| Data; parameters | 9897; 210 | 12 380; 287 |
| $R_1$; w$R_2$ | 0.0317; 0.0799 | 0.0438; 0.1041 |

### Catalytic screening using molecular complexes

In a typical reaction, complex **3** or **4** (0.015 mmol) was dissolved along with KOH (0.060 mmol) and substrate (0.15 mmol) in 2 mL 2-propanol. Naphthalene (0.1 mmol) was added as an internal standard, and the reactor was sealed and heated to the prescribed temperature for the prescribed time under a 100 Watt-equivalent compact fluorescent bulb. At the end of the reaction, a 0.1 mL aliquot was removed and added to a vial containing 10 μL of 1-methylimidazole to quench the reaction. The resulting solution was then diluted with 0.9 mL dichloromethane and was analysed using GC/MS. Response factor curves were constructed for substrates (benzaldehyde, acetophenone and benzophenone) and products (benzyl alcohol, 1-phenylethanol and diphenylmethanol) for quantification purposes.

### Catalytic screening of *in situ* generated complexes

In a typical reaction, $CpFe(CO)_2I$ (0.020 mmol), imidazolium ligand (0.020 mmol), KOH (0.40 mmol), and acetophenone (0.40 mmol) were dissolved in 4 mL 2-propanol. Naphthalene (0.1 mmol) was added as an internal standard, and the reactor was sealed and heated to the prescribed temperature for the prescribed time. At the conclusion of the reaction, a 0.1 mL aliquot was removed and diluted using 0.9 mL dichloromethane. Ten microliters of 1-methylimidazole was added to the resulting solution to completely quench any remaining reactivity. This solution was then injected into a GC/MS to monitor reaction products. Quantification was carried out by constructing response factor curves for acetophenone and 1-phenylethanol. UV-assisted transfer hydrogenation reactions were carried out in an analogous manner using a specially designed micro reactor consisting of a quartz reactor tube and a handheld low-pressure Hg gaseous discharge lamp operating at 254 nm.

## Acknowledgements

This work was supported by the Southeast Partnership for Integrated Biomass Supply Systems, which is supported by Agriculture and Food Research Initiative Competitive Grant no. 2011-68005-30410 from the USDA National Institute of Food and Agriculture. Additional funding was provided by UT Ag Research. The computational results were made possible in part by a grant of high performance computing resources and technical support from the Alabama Supercomputer Authority. The authors are grateful to Dr Craig Barnes (UTK Department of Chemistry) for assistance with FTIR measurements.

## Notes and references


1 R. M. Bullock, in *Catalysis without Precious Metals*, Wiley-VCH Verlag GmbH & Co. KGaA, 2010, pp. I–XVIII.
2 I. Bauer and H.-J. Knölker, *Chem. Rev.*, 2015, **115**, 3170–3387.
3 N. N. Greenwood and A. Earnshaw, in *Chemistry of the Elements*, Butterworth-Heinemann, Oxford, 2nd edn, 1997, pp. 1070–1112.
4 R. Dorta, E. D. Stevens, N. M. Scott, C. Costabile, L. Cavallo, C. D. Hoff and S. P. Nolan, *J. Am. Chem. Soc.*, 2005, **127**, 2485–2495.
5 F. Glorius, in *N-Heterocyclic Carbenes in Transition Metal Catalysis*, Springer, Berlin, Heidelberg, 2007, vol. 21, ch. 1, pp. 1–20.
6 G. Huttner and W. Gartzke, *Chem. Ber.*, 1972, **105**, 2714–2725.
7 K. Öfele and C. G. Kreiter, *Chem. Ber.*, 1972, **105**, 529–540.
8 B. Cetinkaya, P. Dixneuf and M. F. Lappert, *J. Chem. Soc., Chem. Commun.*, 1973, 206.
9 B. Cetinkaya, P. Dixneuf and M. F. Lappert, *J. Chem. Soc., Dalton Trans.*, 1974, 1827–1833.
10 M. J. Ingleson and R. A. Layfield, *Chem. Commun.*, 2012, **48**, 3579–3589.
11 K. Riener, S. Haslinger, A. Raba, M. P. Högerl, M. Cokoja, W. A. Herrmann and F. E. Kühn, *Chem. Rev.*, 2014, **114**, 5215–5272.
12 D. Bézier, J.-B. Sortais and C. Darcel, *Adv. Synth. Catal.*, 2013, **355**, 19–33.
13 J. Zheng, J.-B. Sortais and C. Darcel, *ChemCatChem*, 2014, **6**, 763–766.
14 A. Raba, M. Cokoja, W. A. Herrmann and F. E. Kuhn, *Chem. Commun.*, 2014, **50**, 11454–11457.
15 J. A. Przyojski, K. P. Veggeberg, H. D. Arman and Z. J. Tonzetich, *ACS Catal.*, 2015, **5**, 5938–5946.
16 Y. Liu, L. Wang and L. Deng, *J. Am. Chem. Soc.*, 2016, **138**, 112–115.
17 V. V. K. M. Kandepi, J. M. S. Cardoso, E. Peris and B. Royo, *Organometallics*, 2010, **29**, 2777–2782.
18 J. M. S. Cardoso, A. Fernandes, B. d. P. Cardoso, M. D. Carvalho, L. P. Ferreira, M. J. Calhorda and B. Royo, *Organometallics*, 2014, **33**, 5670–5677.
19 J. M. S. Cardoso and B. Royo, *Chem. Commun.*, 2012, **48**, 4944–4946.
20 T. Hashimoto, S. Urban, R. Hoshino, Y. Ohki, K. Tatsumi and F. Glorius, *Organometallics*, 2012, **31**, 4474–4479.
21 S. Warratz, L. Postigo and B. Royo, *Organometallics*, 2013, **32**, 893–897.
22 H. Li, L. C. Misal Castro, J. Zheng, T. Roisnel, V. Dorcet, J.-B. Sortais and C. Darcel, *Angew. Chem., Int. Ed.*, 2013, **52**, 8045–8049.
23 V. César, L. C. Misal Castro, T. Dombray, J.-B. Sortais, C. Darcel, S. Labat, K. Miqueu, J.-M. Sotiropoulos, R. Brousses, N. Lugan and G. Lavigne, *Organometallics*, 2013, **32**, 4643–4655.
24 D. Bézier, F. Jiang, T. Roisnel, J.-B. Sortais and C. Darcel, *Eur. J. Inorg. Chem.*, 2012, **2012**, 1333–1337.
25 D. Bézier, G. T. Venkanna, J.-B. Sortais and C. Darcel, *ChemCatChem*, 2011, **3**, 1747–1750.
26 L. Mercs, G. Labat, A. Neels, A. Ehlers and M. Albrecht, *Organometallics*, 2006, **25**, 5648–5656.
27 F. Jiang, D. Bézier, J.-B. Sortais and C. Darcel, *Adv. Synth. Catal.*, 2011, **353**, 239–244.
28 D. Bézier, G. T. Venkanna, L. C. M. Castro, J. Zheng, T. Roisnel, J.-B. Sortais and C. Darcel, *Adv. Synth. Catal.*, 2012, **354**, 1879–1884.
29 L. C. M. Castro, J.-B. Sortais and C. Darcel, *Chem. Commun.*, 2012, **48**, 151–153.
30 D. Kumar, A. P. Prakasham, L. P. Bheeter, J.-B. Sortais, M. Gangwar, T. Roisnel, A. C. Kalita, C. Darcel and P. Ghosh, *J. Organomet. Chem.*, 2014, **762**, 81–87.
31 E. Buitrago, F. Tinnis and H. Adolfsson, *Adv. Synth. Catal.*, 2012, **354**, 217–222.
32 A. Volkov, E. Buitrago and H. Adolfsson, *Eur. J. Org. Chem.*, 2013, **2013**, 2066–2070.
33 M. D. Bala and M. I. Ikhile, *J. Mol. Catal. A: Chem.*, 2014, **385**, 98–105.
34 M. T. Zarka, M. Bortenschlager, K. Wurst, O. Nuyken and R. Weberskirch, *Organometallics*, 2004, **23**, 4817–4820.
35 T. I. Gouki Fukata and M. Tashiro, *Heterocycles*, 1981, **16**, 549–554.
36 P. Buchgraber, L. Toupet and V. Guerchais, *Organometallics*, 2003, **22**, 5144–5147.
37 O. Eisenstein and R. H. Crabtree, *New J. Chem.*, 2013, **37**, 21–27.
38 A. Ouali, J.-P. Majoral, A.-M. Caminade and M. Taillefer, *ChemCatChem*, 2009, **1**, 504–509.
39 V. Polshettiwar and R. S. Varma, *Green Chem.*, 2009, **11**, 1313–1316.
40 L. C. M. Castro, D. Bézier, J.-B. Sortais and C. Darcel, *Adv. Synth. Catal.*, 2011, **353**, 1279–1284.
41 T. Matsuura and Y. Kitaura, *Bull. Chem. Soc. Jpn.*, 1968, **41**, 2483–2485.
42 D. K. Liu, R. J. Chin and A. L. Lai, *Chem. Mater.*, 1991, **3**, 13–14.
43 M. J. Frisch, G. W. Trucks, H. B. Schlegel, G. E. Scuseria, M. A. Robb, J. R. Cheeseman, G. Scalmani, V. Barone, B. Mennucci, G. A. Petersson, H. Nakatsuji, M. Caricato, X. Li, H. P. Hratchian, A. F. Izmaylov, J. Bloino, G. Zheng, J. L. Sonnenberg, M. Hada, M. Ehara, K. Toyota, R. Fukuda, J. Hasegawa, M. Ishida, T. Nakajima, Y. Honda, O. Kitao, H. Nakai, T. Vreven, J. A. Montgomery Jr, J. E. Peralta, F. Ogliaro, M. Bearpark, J. J. Heyd, E. Brothers, K. N. Kudin, V. N. Staroverov, R. Kobayashi, J. Normand, K. Raghavachari, A. Rendell, J. C. Burant, S. S. Iyengar, J. Tomasi, M. Cossi, N. Rega, J. M. Millam, M. Klene, J. E. Knox, J. B. Cross, V. Bakken, C. Adamo, J. Jaramillo, R. Gomperts, R. E. Stratmann, O. Yazyev, A. J. Austin, R. Cammi, C. Pomelli, J. W. Ochterski, R. L. Martin, K. Morokuma, V. G. Zakrzewski, G. A. Voth, P. Salvador, J. J. Dannenberg, S. Dapprich, A. D. Daniels, Ö. Farkas, J. B. Foresman, J. V. Ortiz, J. Cioslowski and D. J. Fox, *Gaussian 09, Revision B.01*, Gaussian, Inc., Wallingford CT, 2009.
44 Y. Zhao and D. G. Truhlar, *Acc. Chem. Res.*, 2008, **41**, 157–167.